

*copy 2*



# **THE EFFECT OF PROTON IRRADIATION RATE ON THE SOLAR TRANSMITTANCE OF A THERMAL CONTROL BINDER MATERIAL**

**W. G. Kirby and D. W. Mills, Jr.**

**ARO, Inc.**

**December 1970**

This document has been approved for public release and  
sale; its distribution is unlimited.

**VON KÁRMÁN GAS DYNAMICS FACILITY  
ARNOLD ENGINEERING DEVELOPMENT CENTER  
AIR FORCE SYSTEMS COMMAND  
ARNOLD AIR FORCE STATION, TENNESSEE**

# ***NOTICES***

When U. S. Government drawings specifications, or other data are used for any purpose other than a definitely related Government procurement operation, the Government thereby incurs no responsibility nor any obligation whatsoever, and the fact that the Government may have formulated, furnished, or in any way supplied the said drawings, specifications, or other data, is not to be regarded by implication or otherwise, or in any manner licensing the holder or any other person or corporation, or conveying any rights or permission to manufacture, use, or sell any patented invention that may in any way be related thereto.

Qualified users may obtain copies of this report from the Defense Documentation Center.

References to named commercial products in this report are not to be considered in any sense as an endorsement of the product by the United States Air Force or the Government.

**THE EFFECT OF PROTON IRRADIATION RATE  
ON THE SOLAR TRANSMITTANCE OF A  
THERMAL CONTROL BINDER MATERIAL**

**W. G. Kirby and D. W. Mills, Jr.  
ARO, Inc.**

This document has been approved for public release and  
sale; its distribution is unlimited.

## FOREWORD

The research presented in this report was sponsored by the Arnold Engineering Development Center (AEDC), Air Force Systems Command (AFSC), Arnold Air Force Station, Tennessee, under Program Element 64719F.

The results presented herein were obtained by ARO, Inc. (a subsidiary of Sverdrup & Parcel and Associates, Inc.), contract operator of the AEDC, AFSC, under Contract F40600-71-C-0002. The research was conducted between November 4, 1969, and May 15, 1970, under ARO Project No. SW3005. The manuscript was submitted for publication on October 8, 1970.

This work was discontinued prior to completion of the anticipated program, and this report represents a summary of work accomplished to date. Significant contributions to the experimental work in this report were made by C. R. Williams II and J. V. Waddle.

This technical report has been reviewed and is approved.

Michael G. Buja  
First Lieutenant, USAF  
AF Representative, VKF  
Directorate of Technology

Harry L. Maynard  
Colonel, USAF  
Director of Technology

### ABSTRACT

An experimental investigation was conducted to study the effect of proton irradiation rate on the solar transmittance of a silicone rubber under a  $10^{-8}$  torr vacuum. Measurements were made with 150-kev protons at irradiation rates of  $6.6 \times 10^{10}$ ,  $6.6 \times 10^{11}$ ,  $6.6 \times 10^{12}$ , and  $6.6 \times 10^{13}$  protons/cm<sup>2</sup>/sec, and with 50-kev protons at irradiation rates of  $6.6 \times 10^{11}$  and  $6.6 \times 10^{12}$  protons/cm<sup>2</sup>/sec. The effect of vacuum on the solar transmittance of the test material was negligible. The solar transmittance of the material appeared to decrease with decreasing irradiation rate. The solar transmittance of all samples was a power law function of the total energy accumulated per unit area of the sample between total energy levels of  $10^8$  and  $10^{10}$  ergs/cm<sup>2</sup>/sec.

## CONTENTS

	<u>Page</u>
ABSTRACT . . . . .	iii
I. INTRODUCTION . . . . .	1
II. EXPERIMENTAL APPARATUS . . . . .	1
III. PROCEDURE . . . . .	3
IV. RESULTS AND DISCUSSION . . . . .	4
V. CONCLUDING REMARKS . . . . .	6
REFERENCES . . . . .	7

## APPENDIXES

### I. ILLUSTRATIONS

#### Figure

1. Combined Environment Test Chamber . . . . .	11
2. Schematic of Test System . . . . .	12
3. Sample Holder and Test Samples . . . . .	13
4. Sample Mount . . . . .	14
5. Normalized Solar Transmittance versus Total Energy for 150-keV Protons with $6.6 \times 10^{13}$ Protons/cm <sup>2</sup> -sec Irradiation Rate ( $T = 14.32 E^{-0.142}$ ) . . . . .	16
6. Normalized Solar Transmittance versus Total Energy for 150-keV Protons with $6.6 \times 10^{12}$ Protons/cm <sup>2</sup> -sec Irradiation Rate ( $T = 13.3 E^{-0.138}$ ) . . . . .	17
7. Normalized Solar Transmittance versus Total Energy for 150-keV Protons with $6.6 \times 10^{12}$ Protons/cm <sup>2</sup> -sec Irradiation Rate ( $T = 11.67 E^{-0.131}$ ) . . . . .	18
8. Normalized Solar Transmittance versus Total Energy for 150-keV Protons with $6.6 \times 10^{12}$ Protons/cm <sup>2</sup> -sec Irradiation Rate ( $T = 9.45 E^{-0.123}$ ) . . . . .	19
9. Normalized Solar Transmittance versus Total Energy for 150-keV Protons with $6.6 \times 10^{11}$ Protons/cm <sup>2</sup> -sec Irradiation Rate ( $T = 12.72 E^{-0.139}$ ) . . . . .	20
10. Normalized Solar Transmittance versus Total Energy for 150-keV Protons with $6.6 \times 10^{11}$ Protons/cm <sup>2</sup> -sec Irradiation Rate ( $T = 12.99 E^{-0.140}$ ) . . . . .	21
11. Normalized Solar Transmittance versus Total Energy for 150-keV Protons with $6.6 \times 10^{10}$ Protons/cm <sup>2</sup> -sec Irradiation Rate ( $T = 15.2 E^{-0.148}$ ) . . . . .	22
12. Variation in Solar Transmittance with Irradiation Rate for 50-keV Protons . . . . .	23
13. Normalized Solar Transmittance versus Total Energy for 50-keV Protons with $6.6 \times 10^{12}$ Protons/cm <sup>2</sup> -sec Irradiation Rate ( $T = E = 5.15 E^{-0.0918}$ ) . . . . .	24

<u>Figure</u>	<u>Page</u>
14. Normalized Solar Transmittance versus Total Energy for 50-kev Protons with $6.6 \times 10^{12}$ Protons/cm <sup>2</sup> -sec Irradiation Rate ( $T = 4.97 E^{-0.0894}$ ) . . . . .	25
15. Normalized Solar Transmittance versus Total Energy for 50-kev Protons with $6.6 \times 10^{11}$ Protons/cm <sup>2</sup> -sec Irradiation Rate ( $T = 2.81 E^{-0.0656}$ ) . . . . .	26
16. Variation in Solar Transmittance with Irradiation Rate for 50-kev Protons . . .	27
 II. TABLE	
1. Summary of Test Data . . . . .	28

## **SECTION I INTRODUCTION**

The objective of this work is to evaluate techniques for producing realistic results in ground tests utilizing a simulated, combined environment of space. In general, the need for exact simulation in an environment involving electrons, protons, and electromagnetic radiation in a vacuum will be assessed. Exact simulation of this environment can only be approximated with the current state of the art (Ref. 1); therefore, it is important that problems associated with inexact simulation be identified and evaluated. Problem areas that will influence the degree of simulation necessary are (1) irradiation rate effects - the degree by which ground test rates may exceed those existing in space (Refs. 1 and 2), (2) synergistic effects - effects that occur because all of the constituents of the space environment are not present in the test environment (Refs. 1 and 2), and (3) energy spectrum effects (Ref. 1). The importance of producing the energy spectrum for each type of radiation has not been evaluated basically because irradiation technology has not advanced to the point that these experiments are practical. Since irradiation rate effects could be a factor in any investigation of synergistic and energy spectrum effects, some understanding of irradiation rate effects should be obtained prior to investigating the other problem areas.

The initial investigation of irradiation rates was planned for the passive thermal control surface field. The general approach was to determine if rate effects were significant by studying the change in optical properties of candidate thermal control materials for various irradiation rates of electrons, protons, and electrons plus protons.

This report presents the initial irradiation rate data obtained with protons on a thermal control binder material, silicone rubber. Anticipated extensions of this program would include similar investigation of thermal control pigments, as well as the complete thermal control materials.

## **SECTION II EXPERIMENTAL APPARATUS**

### **2.1 TEST CHAMBER**

The combined environment test chamber is a cylindrical, ultrahigh vacuum chamber of stainless steel construction, 24 in. in diameter and 68.5 in. in height (Figs. 1 and 2, Appendix I). The pumping system for this chamber is of the titanium ion-sublimation type with a speed in excess of 6000 l/sec for air. Located 18 in. below the top of the chamber and spaced 90 deg apart around the chamber circumference are three ports: (1) a 4-in.-diam glass viewing port, (2) a 4-in.-diam glass port for introducing light from a monochromator into an integrating sphere, and (3) an 8-in.-diam port and valve for introducing radiation into the test chamber.

### **2.2 TEST SAMPLE**

The test material is a silicone rubber coating produced by Dow Corning as No. 92-009 dispersion coating. This material has been used extensively as the binding agent for pigments



in thermal control coatings. The test samples were made by curing the dispersion coating in a Teflon<sup>®</sup> mold. The resulting samples were 0.75-in. disks whose thicknesses varied between 0.004 and 0.007 in. The sample thickness was kept within these limits with the following objectives in mind: (1) to make the samples thin enough such that adequate transmission measurement could be obtained on the material, and (2) to make the samples thick enough such that all of the energy of the irradiating particle would be absorbed by the material.

## 2.3 SAMPLE HOLDER

The sample holder (Fig. 3, Ref. 2) is a horizontal 18-in.-diam aluminum plate, 0.5 in. thick, which is suspended from a rotary feedthrough 18 in. from the top of the chamber. A total of 25 sample or test support item positions are spaced evenly around the circumference of the holder. These positions are indexed so that they may be externally positioned in front of the irradiation or spectral transmission station. The test support items include Faraday cups for charged particle detection, beam visualization devices, and reference transmission samples.

The test samples are held in right-angle aluminum mounts (Fig. 4) that are bolted to the sample holder. Each mount can accommodate a sample 1 in. in diameter; however, only a 1/2-in.-diam area is exposed to the irradiating beam. Approximately 1 1/16 in. above the center of the sample is a 3/8-in.-diam hole for the reference light beam to pass into the integrating sphere during spectral transmission measurements. The integrating sphere is translated up to the back side of the sample mount during transmission measurement. The correct position of the sphere relative to the sample is verified by an electrical contact on the sample mount.

## 2.4 TRANSMISSION MEASUREMENT SYSTEM

The spectral transmission system (Fig. 2) consists of (1) the integrating sphere, detectors, and traversing device inside the vacuum chamber; (2) a monochromator and transfer optics from the monochromator to the integrating sphere; and (3) the detector signal preamplifier, amplifier and readout, and a light-beam chopper.

The external shape of the integrating sphere is in the form of a cube in order to facilitate mounting of the detectors and the sphere. The centers of the detector ports and the sample light-beam port are on the same plane and are located 90 deg apart on a circle within this plane. The detector ports are opposite each other and shielded from direct view of light entering the sphere from the sample light port by two elliptical shields positioned on either side of this port. A reference light-beam port in the sphere is 1 1/16 in. above the sample light port. The internal surface of the sphere is coated with barium sulfate. Monochromatic light is produced for the spectral transmission measurement by a properly filtered grating monochromator. The light beam is interrupted by a chopper and transmitted to the sphere by transfer optics. A two-position flip lens sends the monochromatic light into the sphere by passing through either the sample or reference port. The detector signal is relayed to a recorder by a preamplifier and synchronous amplifier.

The spectral transmittance of a sample is obtained from the following relation:

$$T_s = \frac{D_s}{D_s R}$$

where  $D_s$  is the sphere detector output when the light beam passes through the sample into the sphere and  $D_r$  is the detector output when the light beam enters the sphere without passing through the sample. This relationship assumes a uniform and diffuse reflectance of the wall of the sphere, and that light entering the sphere does not go to the detectors without first striking the sphere wall.

## 2.5 PROTON SOURCE

The proton accelerator (Ref. 2) has the capability of producing particles with energies up to 250 kev. The accelerator utilizes a radio frequency ion source with a maximum output of 1 ma which is approximately 85-percent protons. Titanium ion-sublimation pumping is provided at the exit of the accelerator tube and at the entrance to the test chamber. Two magnetic quadrupole lenses focus and direct the test beam to the sample. This source can be isolated from and operated independently of the test chamber in order to facilitate checkout and troubleshooting. This portion of the test hardware is referred to as the radiation injection system.

## 2.6 CHAMBER INSTRUMENTATION

The gas pressure and composition within the test chamber were monitored, respectively, by a hot filament vacuum gage and a residual gas analyzer. Proton beam Faraday cup outputs were measured by a microammeter.

## SECTION III PROCEDURE

The main test chamber was evacuated to below  $5 \times 10^{-8}$  torr, and the background gas content was monitored by a mass spectrometer. Simultaneously, the radiation injection system pressure was reduced to  $5 \times 10^{-7}$  torr. The isolation valve between the main chamber and the radiation injection was opened after this pressure was attained.

The proton beam was activated and allowed to impinge on a quartz viewing disk mounted on the sample holder. A beam impinging on the sample outline on the disk would hit a sample in precisely the same manner when the sample is in turn rotated into the irradiation position. After the proton beam was focused, and the intensity was set, the isolation valve was closed with the proton beam on, and the sample to be irradiated was rotated into position. Then the isolation valve was opened simultaneously with the activation of an irradiation timer. After a desired time of irradiation, the isolation valve was closed, and in situ spectral transmission measurements were made on the sample (Section 2.4). This same procedure was followed until the desired total irradiation time was achieved for each sample.

The in situ measured spectral transmittance was used in a numerical integration process with the solar spectral irradiance (Ref. 3) to obtain the solar transmittance. For the purpose

of numerical integration, the transmittance and solar spectra were divided into  $0.1\text{-}\mu$  intervals over the wavelength region from  $0.4$  to  $2.5\mu$ ,  $0.05\text{-}\mu$  intervals from  $0.3$  to  $0.4\mu$ , and  $0.025\text{-}\mu$  intervals from  $0.225$  to  $0.3\mu$ . The solar transmittance (fraction) was obtained by summing, for all wavelength intervals, the product of the average interval transmittance (fraction) and the fraction of solar energy in the wavelength interval.

## SECTION IV RESULTS AND DISCUSSION

It is important that the effects of deviations from the space environment in ground test facilities be evaluated since, in the interest of more efficient and realistic testing, it is desirable and/or necessary to change some of the environmental parameters. The present experimental program was initiated to determine the feasibility of increasing the irradiation rate of protons above that normally found in space for the purpose of reducing the time required for ground testing. Radiation effects produced by protons are determined by the energy transfer between the proton and the target material. The energy transfer is a function of the material and the proton energy and flux.

The experimental data in this report present the change in spectral transmittance of a silicone rubber at a constant proton energy for various irradiation rates. The evaluation is performed at a constant proton energy since the energy transfer and hence the range of penetration of the particle into the material is a function of the particle energy. By this approach, an approximately constant volume of damaged material is being measured for transmittance as a function of irradiation rate. Unfortunately, the energy transfer from the proton to the material cannot be calculated for the energy range of these experiments; consequently, neither the range of the particle nor the probability of damaging a light transmission site may be treated theoretically. This is because the charge exchange process of the proton in this energy range (50 to 150 kev) is not currently understood (Refs. 4 and 5). Above this energy range the form of the energy transfer curve may be calculated, however, the constants of these equations must still be determined experimentally. For rough calculation, empirically determined range equations are of the following form (Refs. 5, 6, 7 and 8):

$$R = CE^x$$

where  $R$  is the particle range for a given particle and material,  $E$  is the particle energy, and  $C$  and  $x$  are experimentally determined constants. For high, nonrelativistic energies,  $x$  approaches 2 as a limiting value, and decreases with decreasing particle energy. From this relation the energy loss per unit path length is of the following form:

$$\frac{dE}{dR} = \frac{1}{x C E^{x-1}}$$

In the absence of an exact range theory and a theory for the change in transmittance with irradiation, the experimental data in this report are plotted to see if a relationship similar to the empirical range equation applies to the change in transmittance with total energy deposited per unit area of the sample. Data are presented for a particle energy

of 150 kev and a flux of  $10^{10}$ ,  $10^{11}$ ,  $10^{12}$ , and  $10^{13}$  protons/cm<sup>2</sup>-sec and 50-kev particle energy with a flux of  $10^{11}$  and  $10^{12}$  protons/cm<sup>2</sup>-sec.

#### 4.1 VACUUM EFFECTS

In order to evaluate the effect of protons on the test samples, it is essential that the effects produced by exposure to vacuum be negligible or known. A reference sample exposed only to vacuum showed a 2.2-percent decrease in measured transmittance after 2520 hr in this environment. The maximum irradiation time with protons during this series of test was 55 hr and 35 min. Consequently, it can be concluded that during all the irradiations test the change in the sample transmittance because of vacuum exposure was negligible.

#### 4.2 IRRADIATION RATE EFFECTS

The irradiation rate effects data in this report were obtained at two energy levels, 150 and 50 kev, and at irradiation rates that were in the  $10^{10}$  to  $10^{13}$  protons/cm<sup>2</sup>-sec range. The intent of this work was to explore the possibility of rate effects at relatively high rates in order to avoid extremely long run times, and to continue this work in the future at lower rates should there be a significant problem.

##### 4.2.1 Irradiation Rate Results with 150-kev Protons

Transmittance data were obtained on silicone rubber samples with 150-kev protons at irradiation rates of  $6.6 \times 10^{10}$ ,  $6.6 \times 10^{11}$ ,  $6.6 \times 10^{12}$ , and  $6.6 \times 10^{13}$  protons/cm<sup>2</sup>-sec. These data are shown in Figs. 5 through 11 as the variation in transmittance with total energy per unit area accumulated on the sample. A normalized transmittance is used in these plots in an attempt to eliminate differences in the data because of variations in the initial transmittance of the samples. A comparison of the data obtained on different samples under identical experimental conditions (Figs. 6, 7, and 8; Figs. 9 and 10; Figs. 13 and 14) indicates that the reproducibility of the samples and systems was good. A summary of all experimental data is shown in Table I (Appendix II).

These plots (Figs. 5 through 11) show that the decrease in transmittance as a function of total energy per unit area irradiated on the sample follows the relationship

$$T = AE^{-x}$$

where  $T$  is the normalized transmittance,  $E$  is the energy per unit area received by the sample, and  $A$  and  $x$  are experimentally determined constants. This relation is valid for values of  $E$  between  $10^8$  and  $10^{10}$  ergs/cm<sup>2</sup>. The transmittance must approach 1.0 below  $E = 10^8$  ergs/cm<sup>2</sup>, and it cannot be predicted how far above  $E = 10^{10}$  ergs/cm<sup>2</sup> that the transmittance will follow this relationship. A given equation can only apply for a given particle energy, since the magnitude of the particle energy effect is not known and cannot be evaluated from present data. The equations for each sample are in Table I and on each plot. A relationship that holds for all data within approximately  $\pm 5$  percent is as follows:

$$T = 11.78 E^{-0.134}$$

where  $T$  and  $E$  are as previously defined. Since all of the data can be represented this closely by a single equation, it is obvious that if there is a rate effect it is relatively small.

In order to determine if there is a rate effect trend with the present data, the calculated normalized transmittance has been plotted as a function of the irradiation rate for two arbitrary values of the total energy,  $10^9$  and  $10^{11}$  ergs/cm<sup>2</sup> (Fig. 12). The trend indicated by these plots is that the increment of decrease in the solar transmittance increases with decreasing rate. Further experimental data are needed at lower rates to determine the extent of this effect.

#### 4.2.2 Irradiation Rate Results with 50-kev Protons

Very limited data were obtained with 50-kev protons, at two rates,  $6.6 \times 10^{11}$  and  $6.6 \times 10^{12}$  protons/cm<sup>2</sup>-sec. These data are plotted in the same manner as the 150-kev data in Figs. 13 through 16. The results are basically the same: (1) the transmittance follows the relationship,  $T = AE^{-x}$  where  $T$ ,  $E$ ,  $A$ , and  $x$  are as previously defined in Section 4.2.1 and (2) the rate trend is similar; the degradation of transmittance increases with decreasing rate. As in Section 4.2.1, these equations should only be utilized within the range of experimental values presented in this report. Figure 15 illustrates this very nicely in the low energy range. The dashed line curve above  $E = 10^8$  ergs/cm<sup>2</sup> corresponds to the applicable region of the above relationship, and the equation for this region is comparable to the other equations for this energy.

One aspect of the 50-kev data that differs from the 150-kev data is the rate of change of transmittance with total accumulated energy. The 50-kev transmittance does not appear to decrease as fast as the transmittance from the 150-kev data. This is probably an indication of the effect of particle energy, but there is insufficient experimental evidence to evaluate this problem in this report.

## SECTION V CONCLUDING REMARKS

The primary objective of the work in this report was to investigate the possibility of irradiation rate effects with protons on a thermal control binder material, a silicone rubber. These evaluations were carried out at a constant particle energy, since the reaction cross section for this material may be a function of the particle energy. The change in solar transmittance with irradiation rate was the basis for evaluating the rate effect. The results of this investigation are summarized in the following statements:

1. The trend in the data suggests a rate effect such that the largest decrease in solar transmittance is obtained with the lowest irradiation rate for a given accumulated energy on the silicone rubber sample.
2. The degradation of the solar transmittance with proton irradiation follows the relationship  $T = AE^{-x}$  between values of the total accumulated energy on the sample of  $10^8$  and  $10^{10}$  ergs/cm<sup>2</sup>.  $T$  is the solar transmittance,

E is the total accumulated energy on the sample, and A and x are empirically determined constants.

3. Irradiation rate studies at much lower rates will be necessary to determine the extent and nature of the rate effects trend presented in this report.

## REFERENCES

1. Kirby, W. G. and Kindall, S. M. "Problems in the Laboratory Simulation of Space Particulate Radiation." AEDC-TR-66-131 (AD804214), December 1966.
2. Kirby, W. G. and Warren, C. N. "Initial Results from a Combined Space Environment Effects Chamber." AEDC-TR-68-139 (AD675551), October 1968.
3. U. S. Air Force Cambridge Research Laboratories. Handbook of Geophysics and Space Environments. Washington, 1965.
4. Bethe, H. A. and Ashkin, J. "Passage of Radiations through Matter," Experimental Nuclear Physics. John Wiley and Sons, Inc., 1953.
5. Seitz, F. and Kochler, J. S. "Displacement of Atoms During Irradiation," Solid State Physics. Volume 2, Academic Press, Inc., 1956.
6. Allesen, S. K. and Warshaw, S. D. "Passage of Heavy Particles through Matter," Reviews of Modern Physics, Volume 15, No. 4, October 1953.
7. Ritson, D. M. Techniques of High Energy Physics. Interscience Publishers, Inc., New York, 1961.
8. Dienes, G. J. and Vineyard, G. H. Radiation Effects in Solids. Volume II, Interscience Publishers, Inc., New York, 1957.

**APPENDIXES**  
**I. ILLUSTRATIONS**  
**II. TABLE**

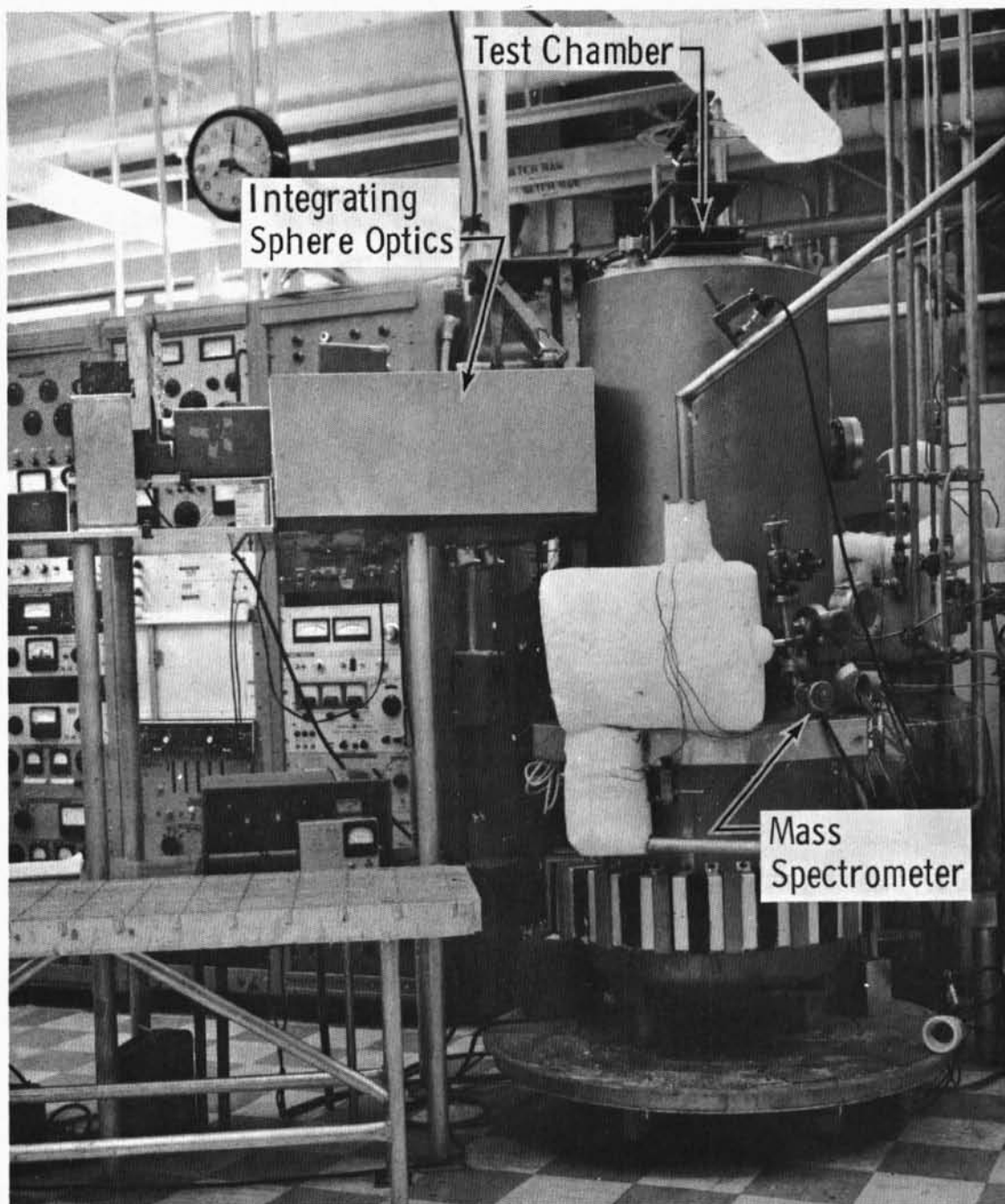


Fig. 1 Combined Environment Test Chamber



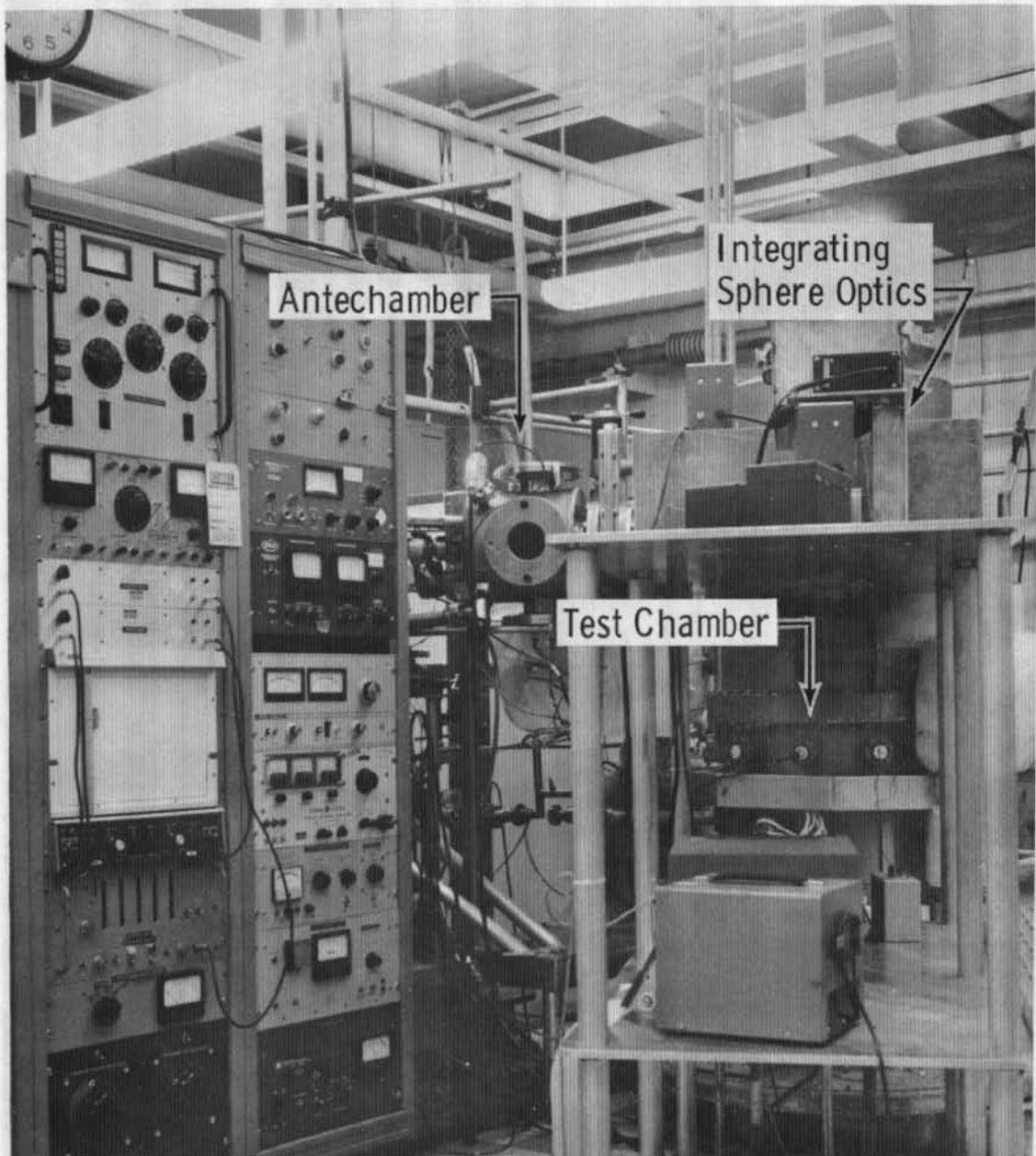


Fig. 1 Concluded

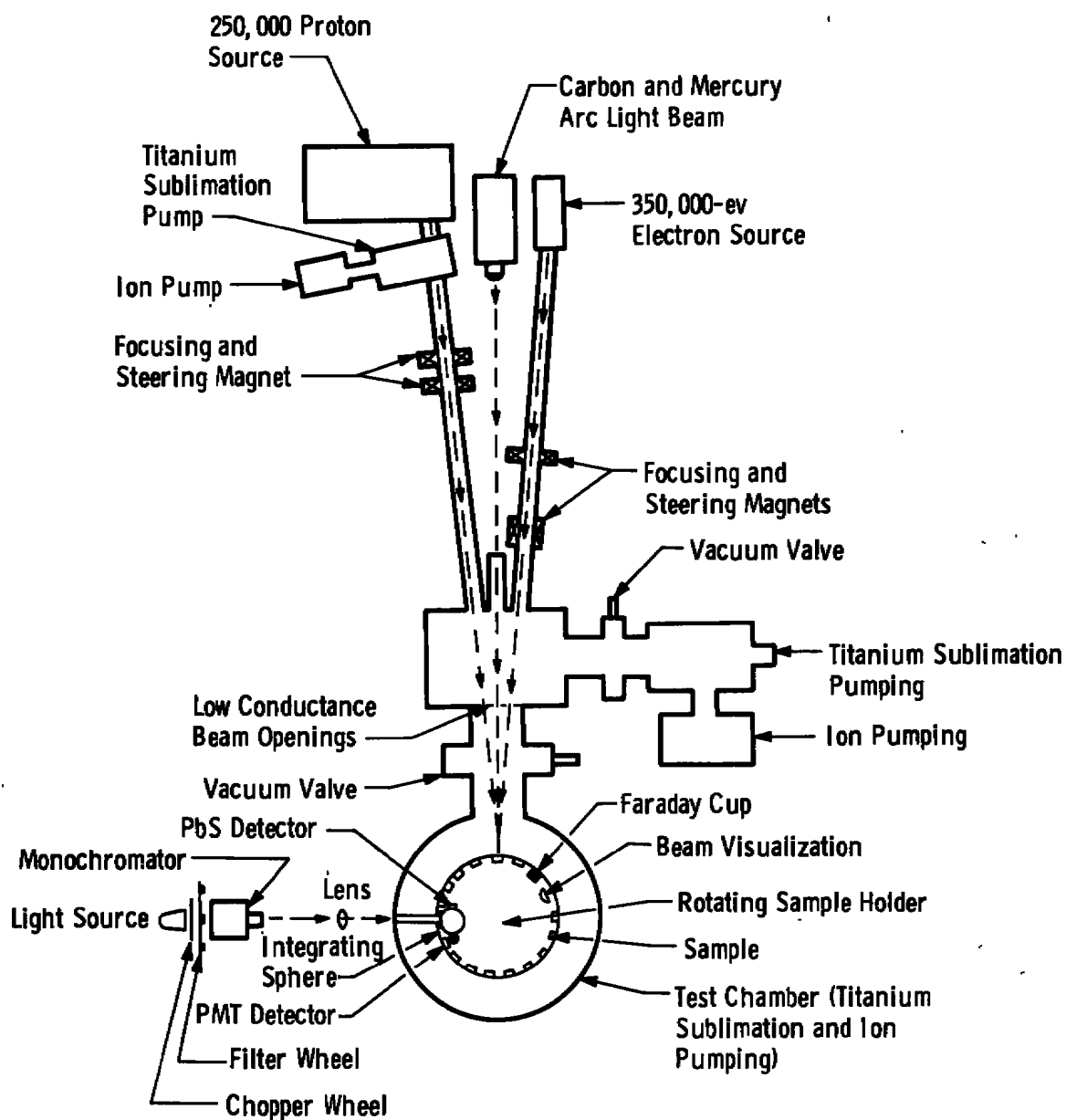


Fig. 2 Schematic of Test System

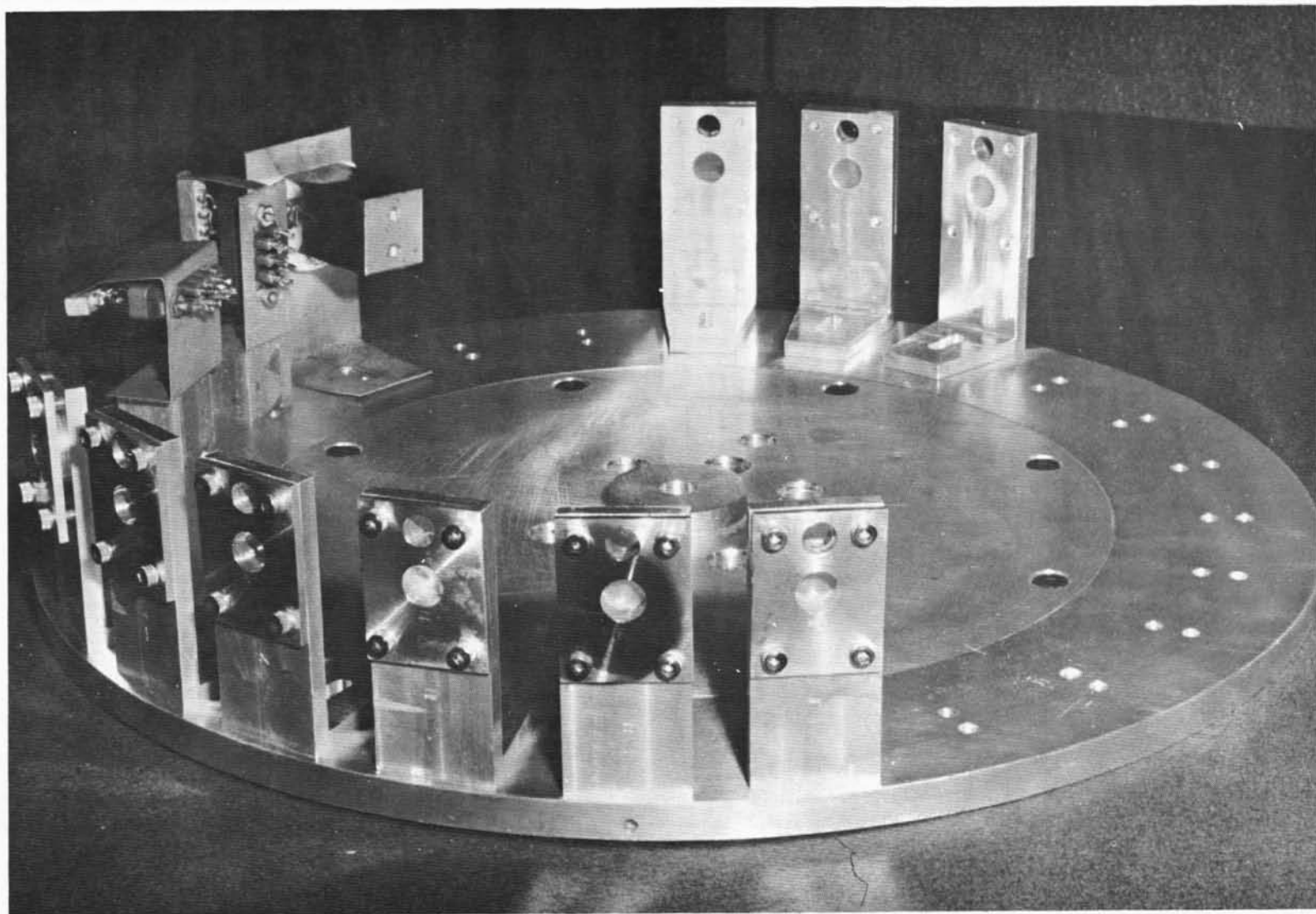


Fig. 3 Sample Holder and Test Samples

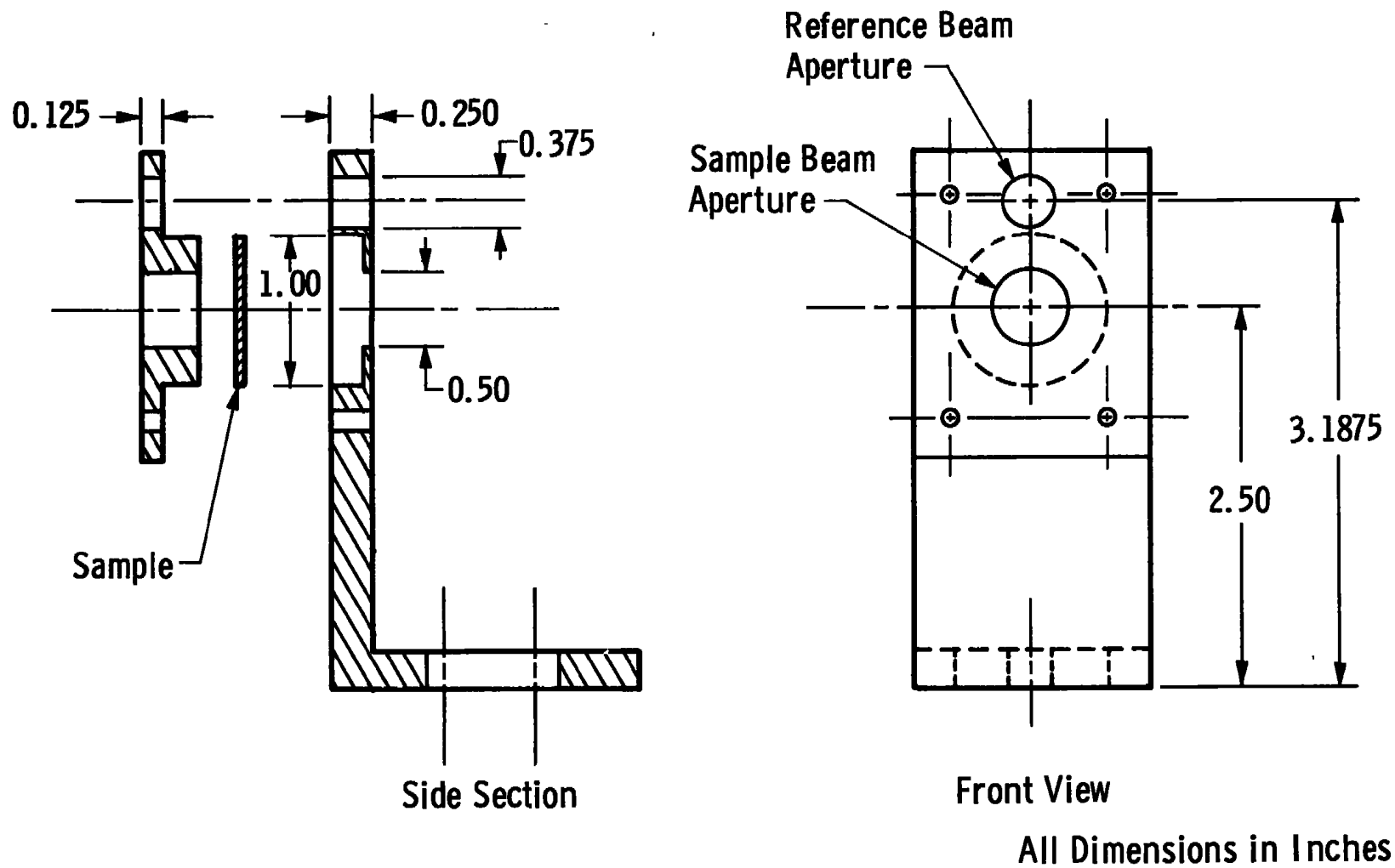


Fig. 4 Sample Mount

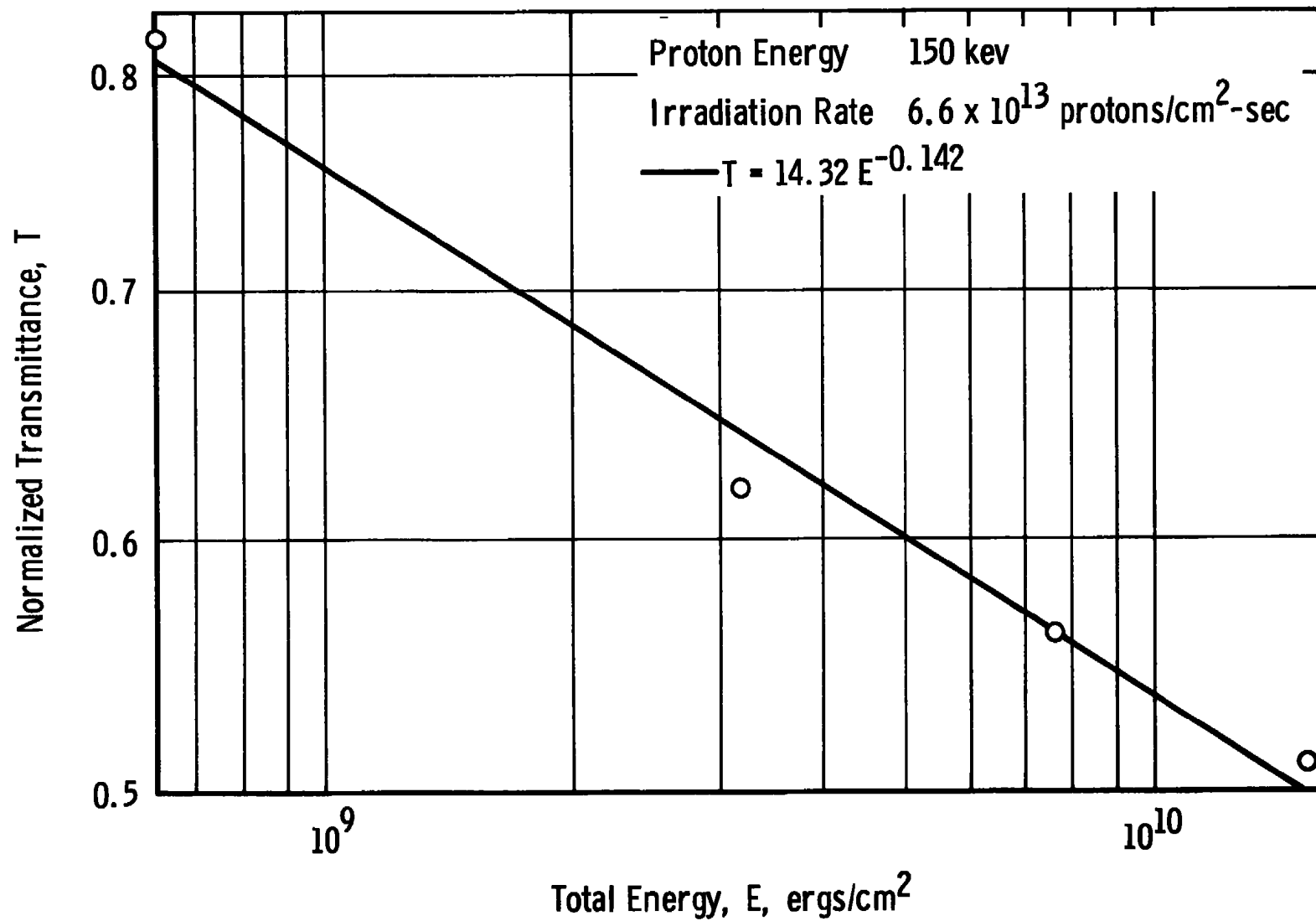


Fig. 5 Normalized Solar Transmittance versus Total Energy for 150-keV Protons with  $6.6 \times 10^{13}$  Protons/cm<sup>2</sup>-sec Irradiation Rate ( $T = 14.32 E^{-0.142}$ )

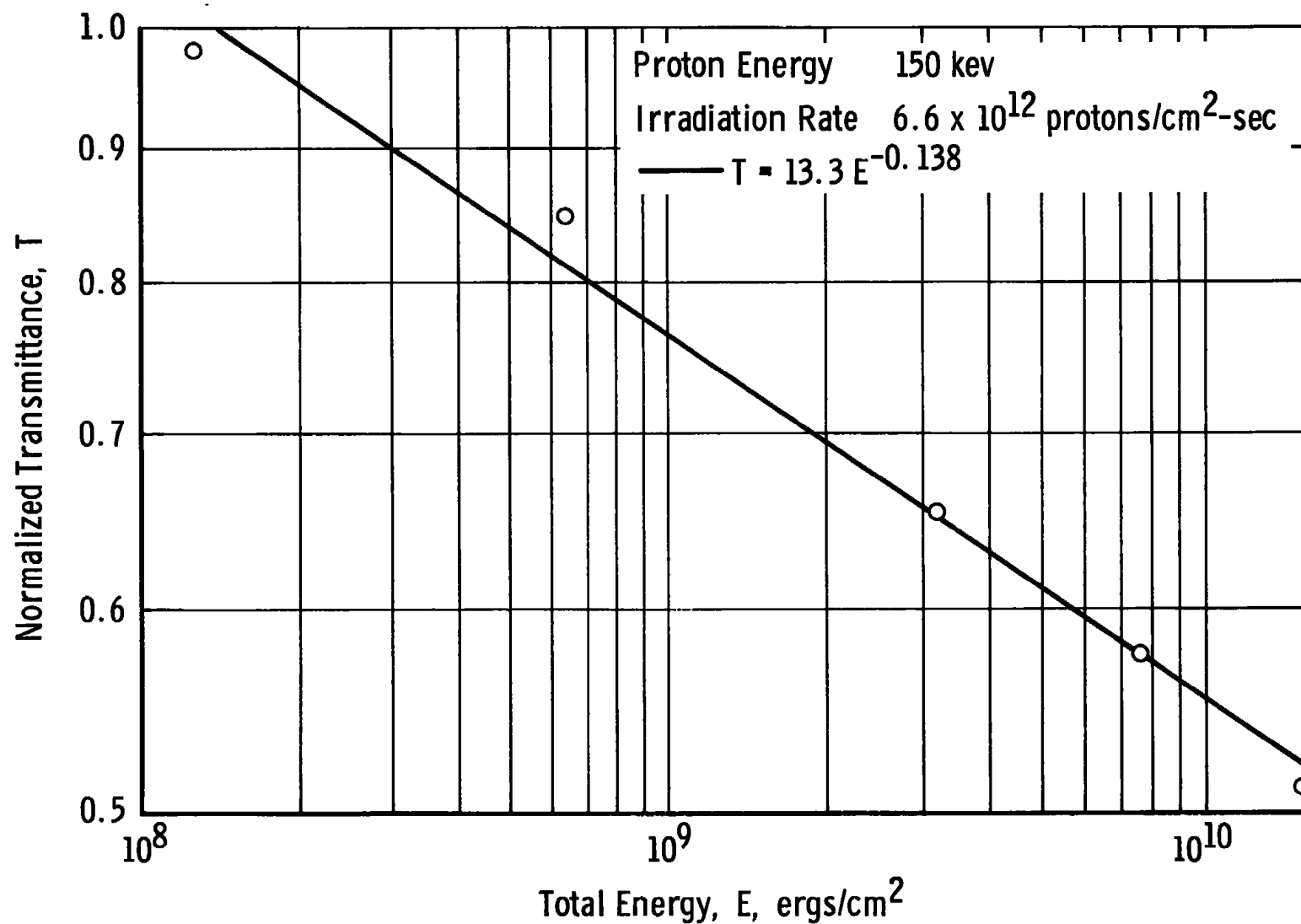


Fig. 6 Normalized Solar Transmittance versus Total Energy for 150-kev Protons with  $6.6 \times 10^{12}$  Protons/cm<sup>2</sup>-sec Irradiation Rate ( $T = 14.32 E^{-0.138}$ )

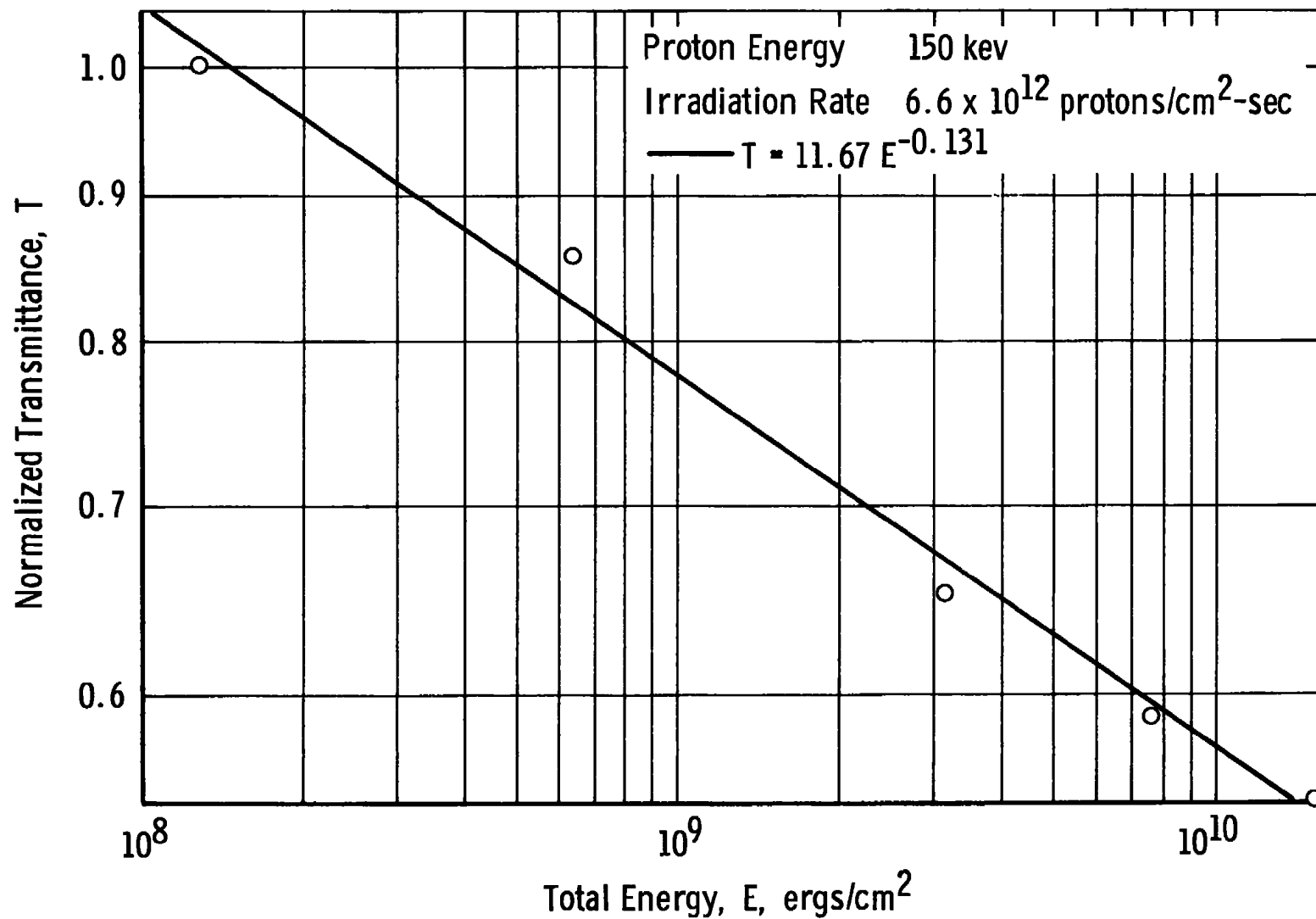


Fig. 7 Normalized Solar Transmittance versus Total Energy for 150-keV Protons with  $6.6 \times 10^{12}$  Protons/cm<sup>2</sup>-sec Irradiation Rate ( $T = 11.67 E^{-0.131}$ )

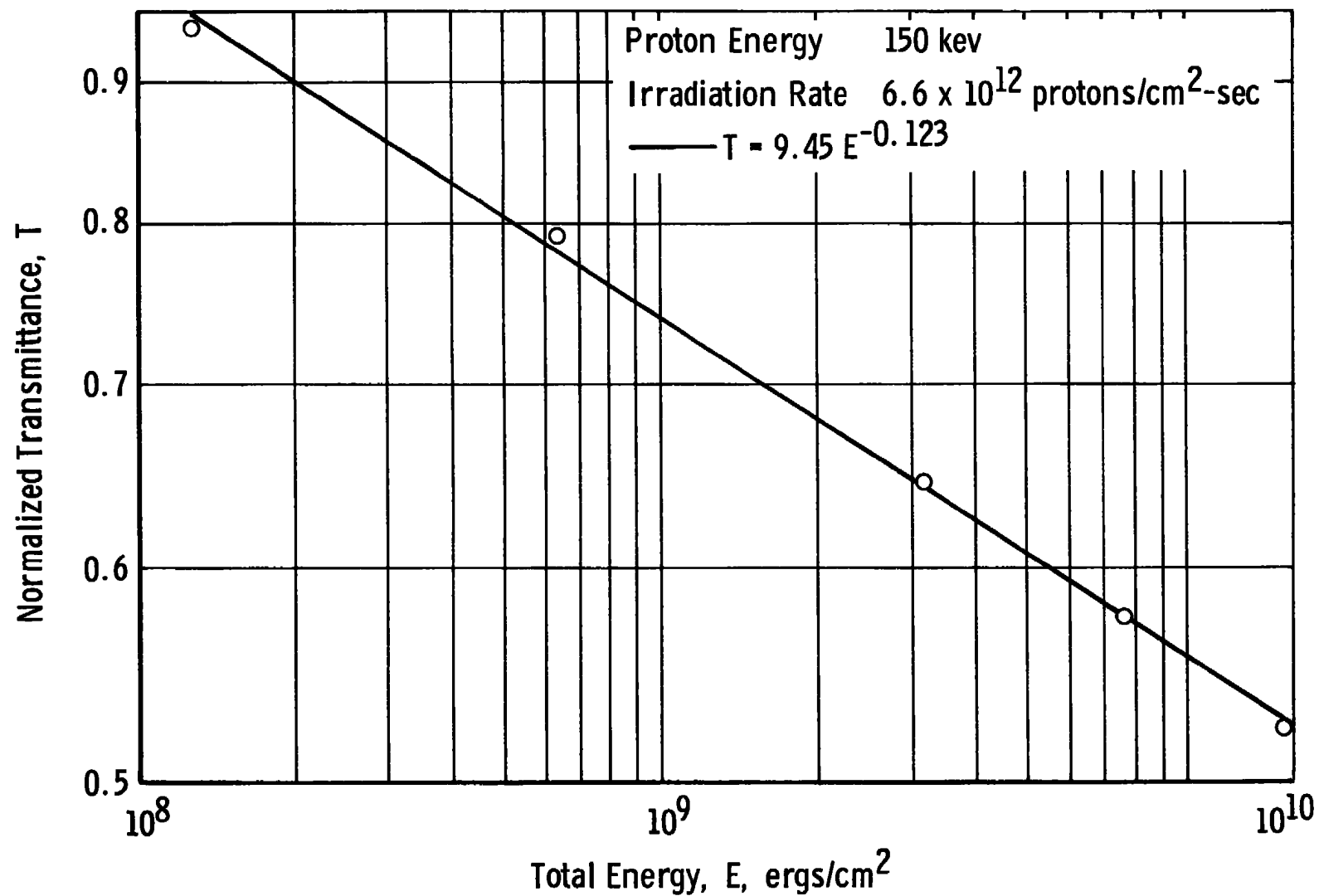


Fig. 8 Normalized Solar Transmittance versus Total Energy for 150-keV Protons with  $6.6 \times 10^{12}$  Protons/cm<sup>2</sup>-sec Irradiation Rate ( $T = 9.45 E^{-0.123}$ )



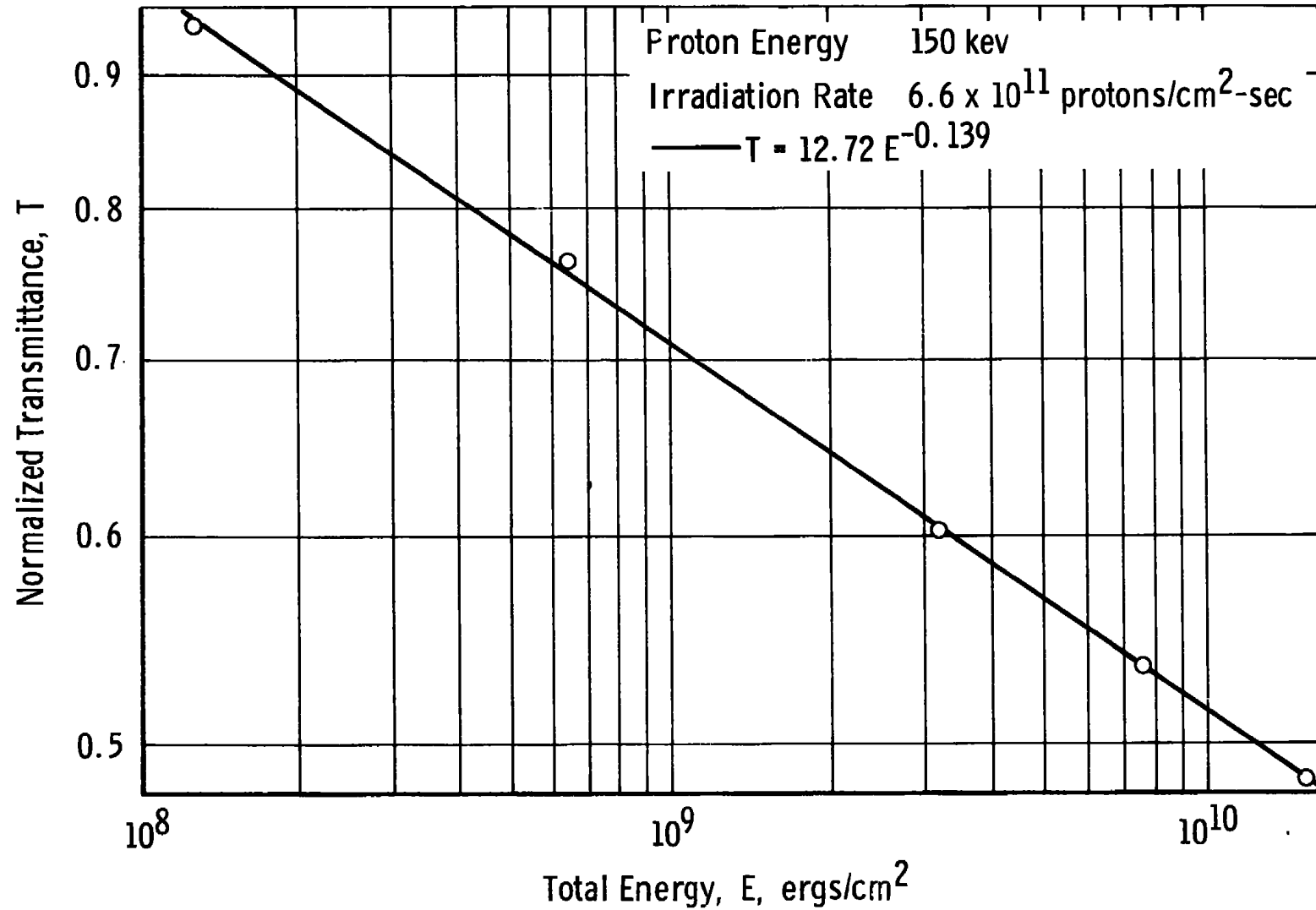


Fig. 9 Normalized Solar Transmittance versus Total Energy for 150-kev Protons with  $6.6 \times 10^{11}$  Protons/cm<sup>2</sup>-sec Irradiation Rate ( $T = 12.72 E^{-0.139}$ )

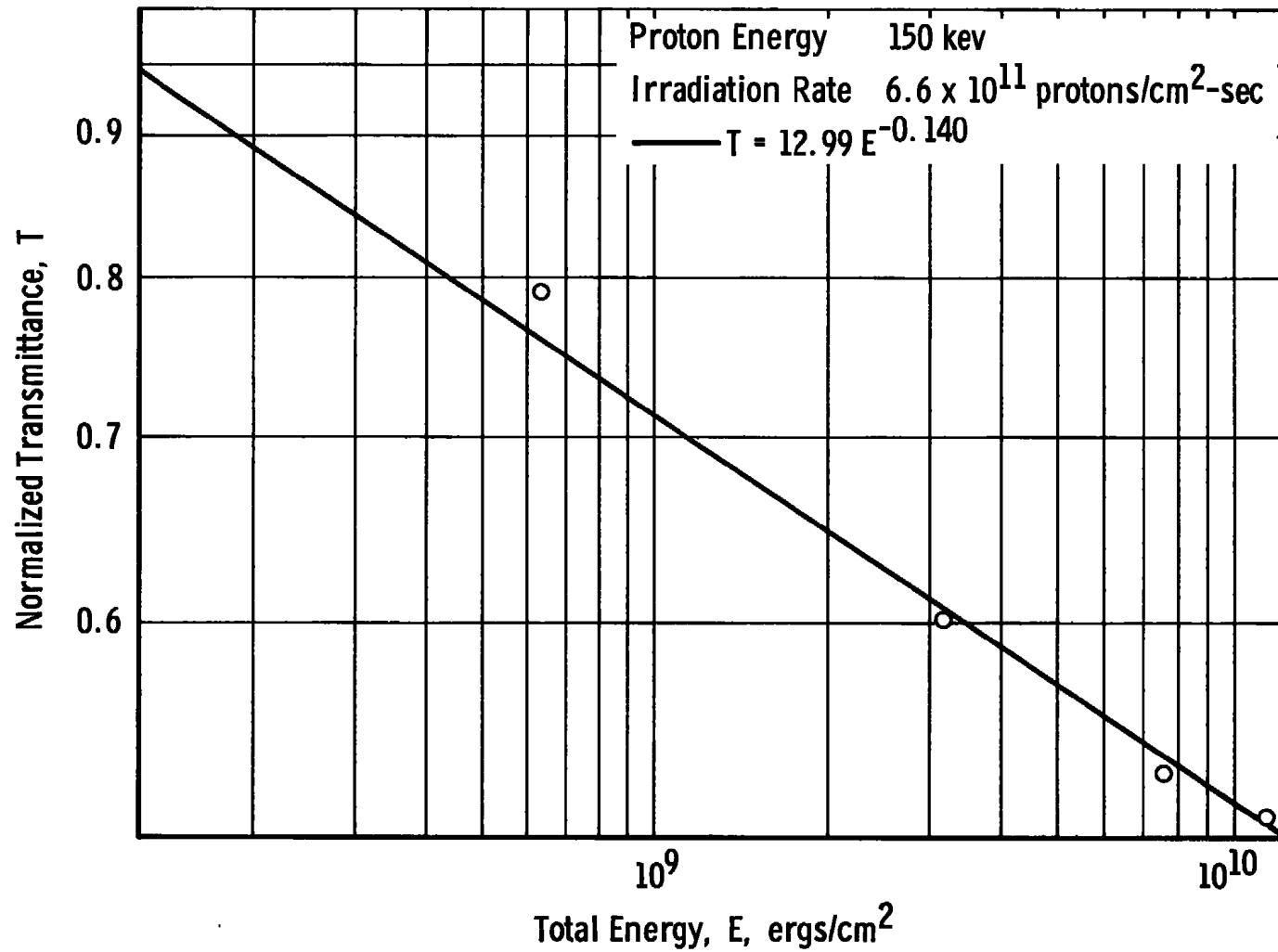


Fig. 10 Normalized Solar Transmittance versus Total Energy for 150-kev Protons with  $6.6 \times 10^{11}$  Protons/cm<sup>2</sup>-sec Irradiation Rate ( $T = 12.99 E^{-0.140}$ )

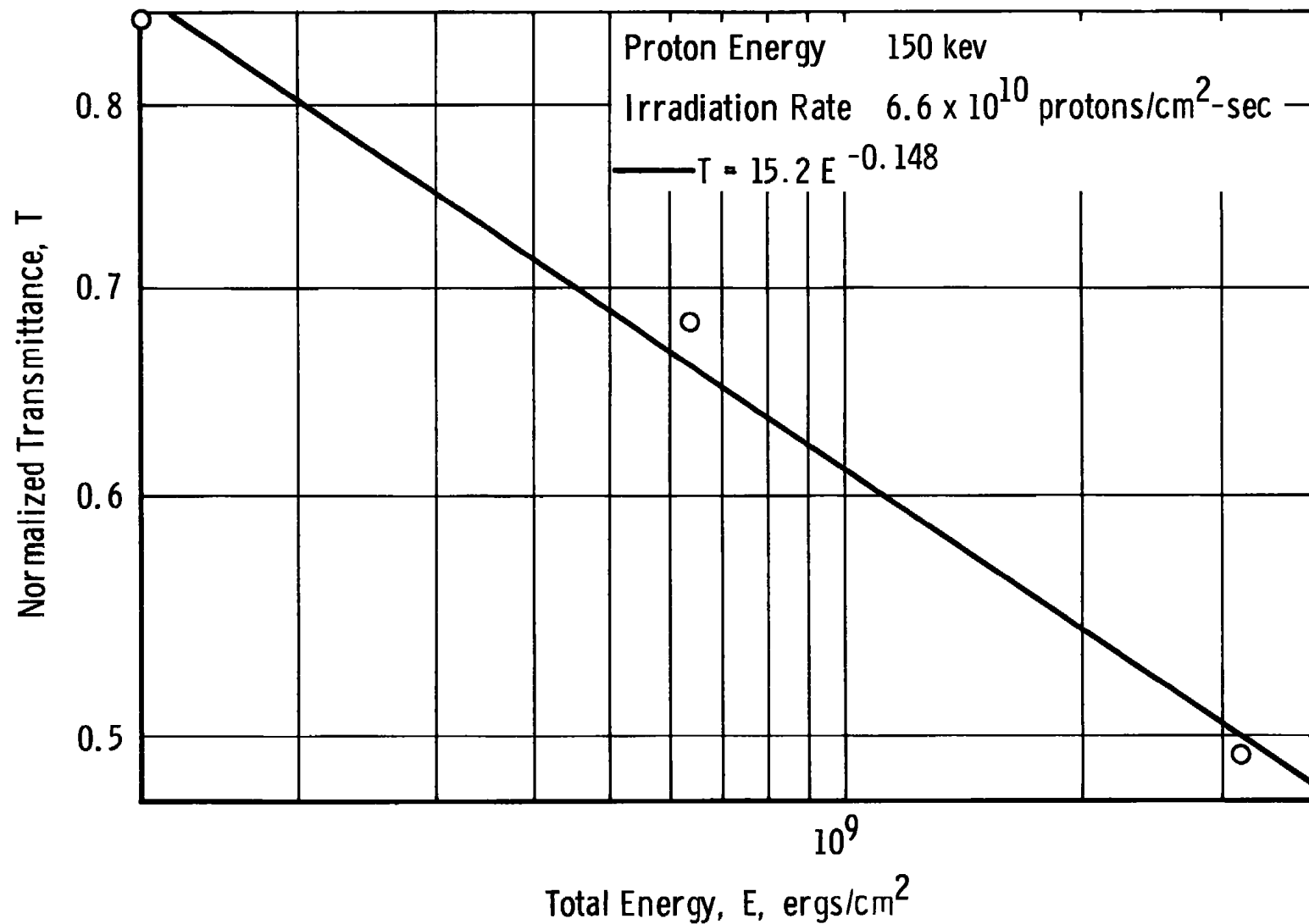


Fig. 11 Normalized Solar Transmittance versus Total Energy for 150-kev Protons with  $6.6 \times 10^{10}$  Protons/cm<sup>2</sup>-sec Irradiation Rate ( $T = 15.2 E^{-0.148}$ )

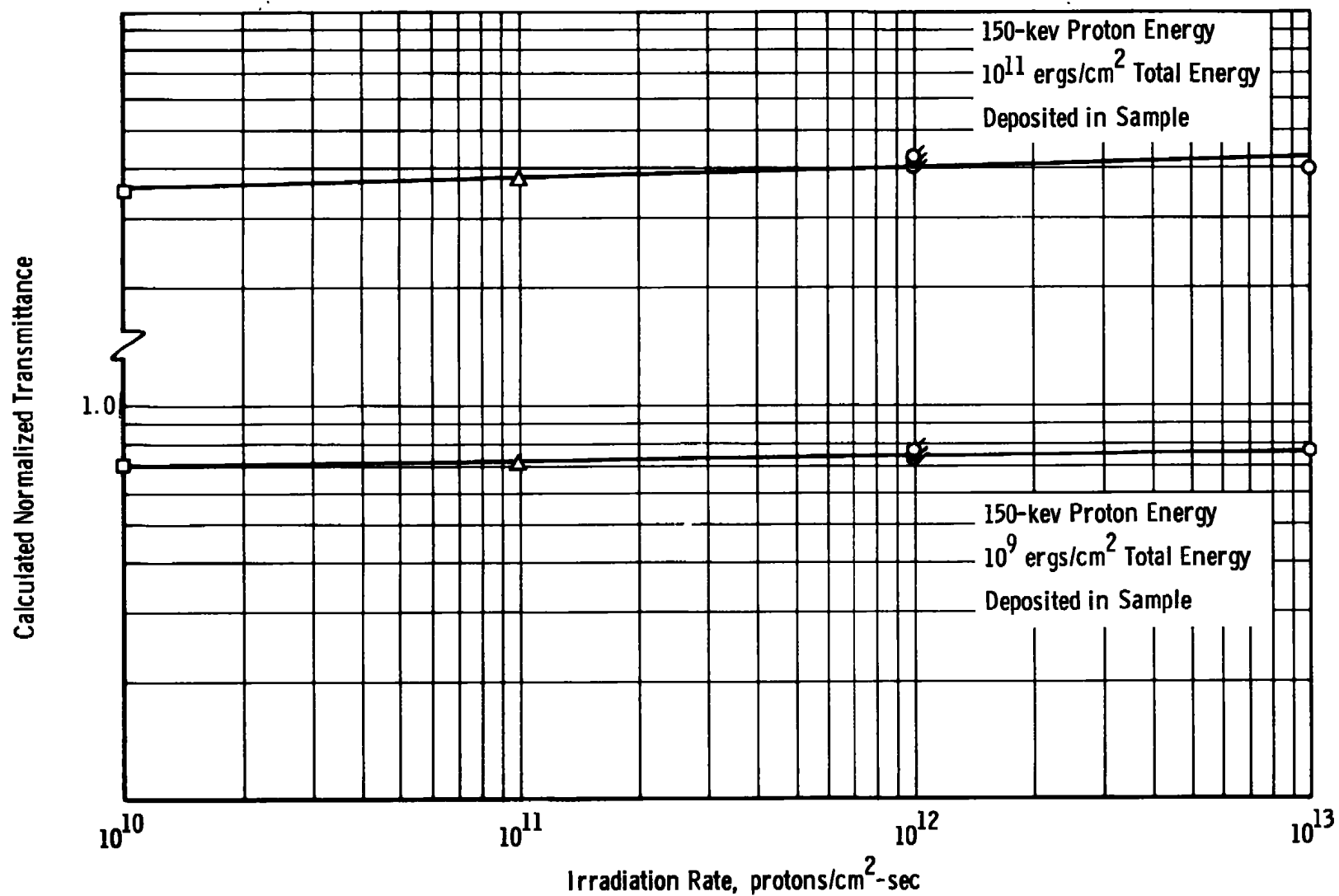


Fig. 12 Variation in Solar Transmittance with Irradiation Rate for 50-kev Protons

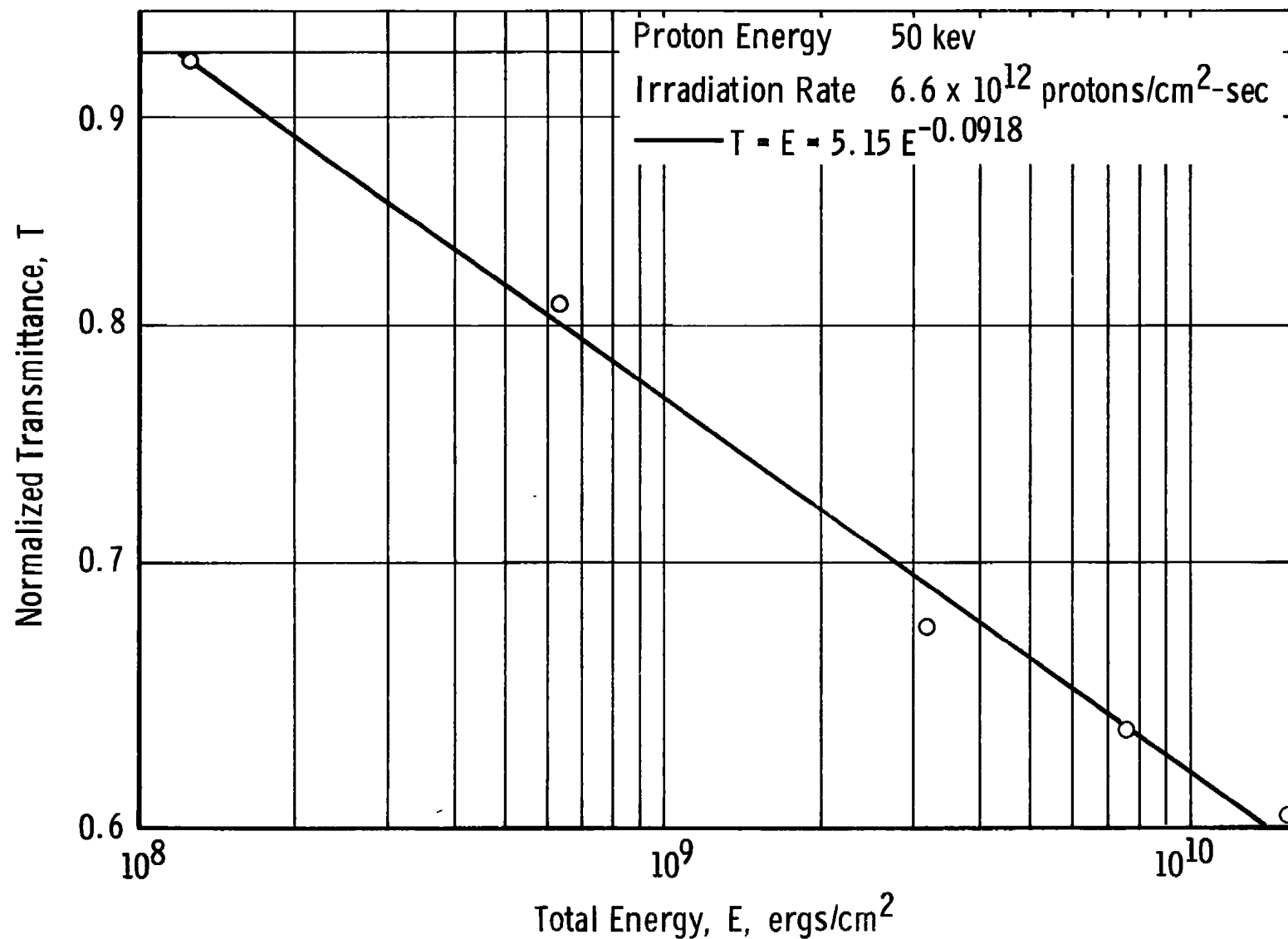


Fig. 13 Normalized Solar Transmittance versus Total Energy for 50-kev Protons with  $6.6 \times 10^{12}$  Protons/cm<sup>2</sup>-sec Irradiation Rate ( $T = E = 5.15 E^{-0.0918}$ )

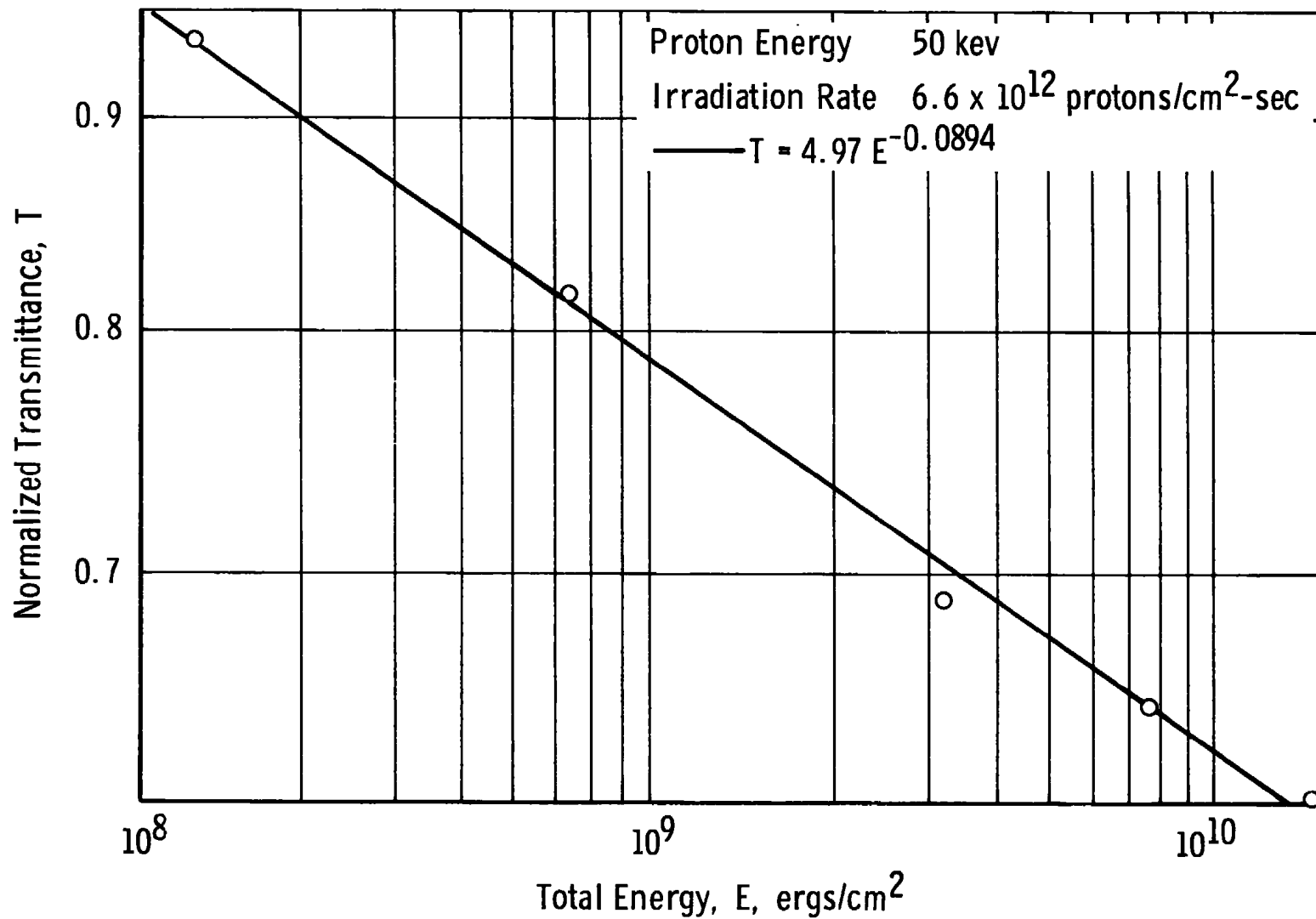


Fig. 14 Normalized Solar Transmittance versus Total Energy for 50-keV Protons with  $6.6 \times 10^{12}$  Protons/cm<sup>2</sup>-sec Irradiation Rate ( $T = 4.97 E^{-0.0894}$ )

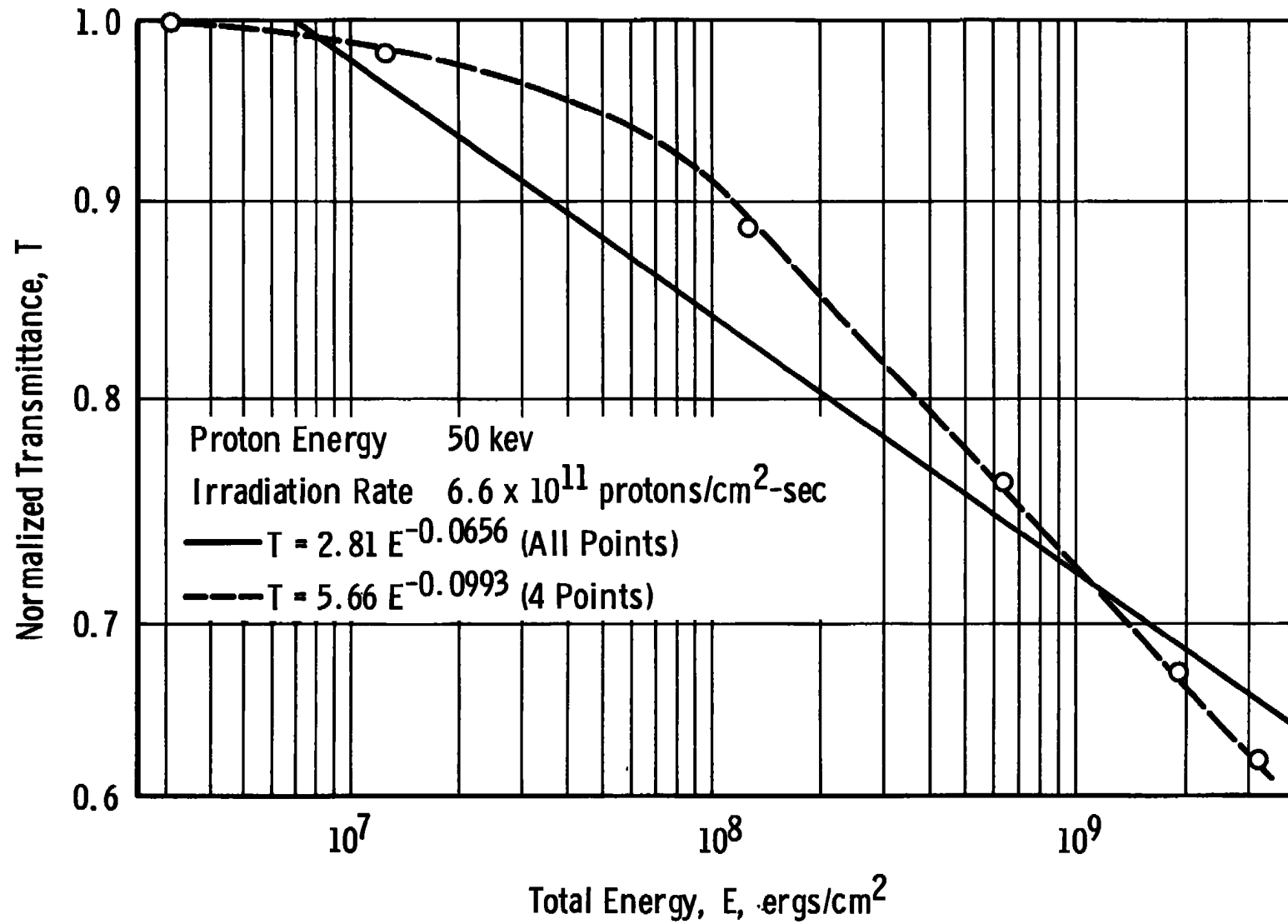


Fig. 15 Normalized Solar Transmittance versus Total Energy for 50-kev Protons with  $6.6 \times 10^{11}$  Protons/cm<sup>2</sup>-sec Irradiation Rate ( $T = 2.81 E^{-0.0656}$ )

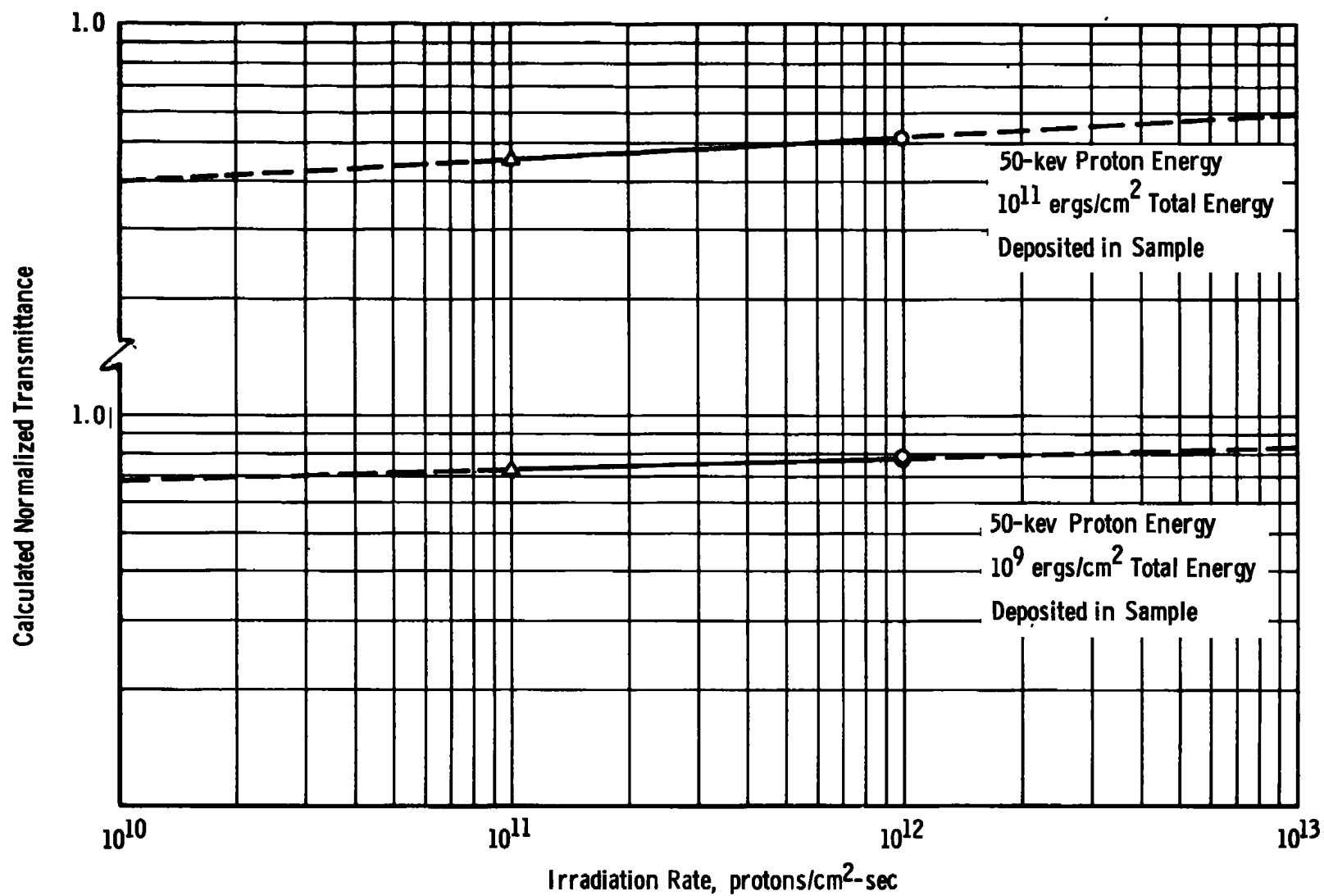


Fig. 16 Variation in Solar Transmittance with Irradiation Rate for 50-kev Protons



**TABLE I**  
**SUMMARY OF TEST DATA**

Figure	Proton Energy	Irradiation Rate	Irradiation Time	Solar Transmittance	Normalized Solar Transmittance	Total Energy (E)	Least Squares Equation
	kev	protons/cm <sup>2</sup> sec	hr, min, sec	(T)	(T)	ergs/cm	
5	150	$6.6 \times 10^{13}$	00:00:00	0.759	1.000	0	$T = 14.32 E^{-0.142}$
			00:00:40	0.622	0.819	$6.36 \times 10^8$	
			00:03:20	0.469	0.618	$3.18 \times 10^9$	
			00:08:00	0.429	0.565	$7.63 \times 10^9$	
			00:16:00	0.396	0.522	$1.53 \times 10^{10}$	
6	150	$6.6 \times 10^{12}$	00:00:00	0.892	1.000	0	$T = 13.3 E^{-0.138}$
			00:01:20	0.876	0.982	$1.27 \times 10^8$	
			00:06:40	0.756	0.847	$6.36 \times 10^8$	
			00:33:20	0.582	0.653	$3.18 \times 10^9$	
			01:20:00	0.514	0.576	$7.63 \times 10^9$	
7	150	$6.6 \times 10^{12}$	02:40:00	0.458	0.513	$1.53 \times 10^{10}$	$T = 11.57 E^{-0.131}$
			00:00:00	0.845	1.000	0	
			00:01:20	0.847	1.002	$1.27 \times 10^8$	
			00:06:40	0.724	0.858	$6.36 \times 10^8$	
			00:33:20	0.550	0.652	$3.15 \times 10^9$	
8	150	$6.6 \times 10^{12}$	01:20:00	0.498	0.590	$7.63 \times 10^9$	$T = 9.45 E^{-0.123}$
			02:40:00	0.466	0.552	$1.53 \times 10^{10}$	
			00:00:00	0.806	1.000	0	
			00:01:20	0.760	0.943	$1.27 \times 10^8$	
			00:06:40	0.638	0.792	$6.36 \times 10^8$	
9	150	$6.6 \times 10^{11}$	00:33:20	0.519	0.644	$3.18 \times 10^9$	$T = 12.72 E^{-0.139}$
			01:20:00	0.464	0.576	$7.63 \times 10^9$	
			02:40:00	0.423	0.525	$1.53 \times 10^{10}$	
			00:00:00	0.888	1.000	0	
			00:13:20	0.836	0.941	$1.27 \times 10^8$	
10	150	$6.6 \times 10^{11}$	01:06:40	0.678	0.763	$6.36 \times 10^8$	$T = 12.99 E^{-0.140}$
			05:33:20	0.535	0.603	$3.18 \times 10^9$	
			13:20:00	0.475	0.535	$7.63 \times 10^9$	
			26:40:00	0.431	0.485	$1.53 \times 10^{10}$	
			00:00:00	0.872	1.000	0	
11	150	$6.6 \times 10^{10}$	00:13:20	0.813	0.932	$1.27 \times 10^8$	$T = 15.2 E^{-0.148}$
			21:06:40	0.689	0.750	$6.36 \times 10^8$	
			05:33:20	0.524	0.601	$3.18 \times 10^9$	
			13:20:00	0.461	0.529	$7.63 \times 10^9$	
			20:00:00	0.445	0.510	$1.15 \times 10^{10}$	
13	50	$6.6 \times 10^{12}$	00:00:00	0.880	1.000	0	$T = 5.15 E^{-0.0918}$
			02:13:20	0.838	0.852	$1.27 \times 10^8$	
			11:06:40	0.688	0.782	$6.36 \times 10^8$	
			55:33:20	0.521	0.592	$3.18 \times 10^9$	
			00:00:00	0.821	1.000	0	
14	50	$6.6 \times 10^{12}$	00:04:00	0.763	0.929	$1.27 \times 10^8$	$T = 4.97 E^{-0.0894}$
			00:20:00	0.664	0.809	$6.36 \times 10^8$	
			01:40:16	0.553	0.674	$3.18 \times 10^9$	
			04:00:00	0.522	0.636	$7.63 \times 10^9$	
			08:00:00	0.498	0.606	$1.53 \times 10^{10}$	
15	50	$6.6 \times 10^{11}$	00:00:00	0.862	1.000	0	$T = 5.66 E^{-0.0993}$
			00:04:30	0.610	0.940	$1.27 \times 10^8$	
			00:20:00	0.703	0.816	$6.36 \times 10^8$	
			01:40:00	0.594	0.689	$3.18 \times 10^9$	
			04:00:00	0.560	0.650	$7.63 \times 10^9$	
		*	08:00:00	0.533	0.618	$1.53 \times 10^{10}$	$T = 2.81 E^{-0.0656}$ (All Points)
			00:00:00	0.263	1.000	0	
			00:01:00	0.863	1.000	$3.18 \times 10^6$	
			00:04:00	0.854	0.990	$1.27 \times 10^7$	
			00:40:00	0.762	0.883	$1.27 \times 10^8$	
		*	03:20:00	0.655	0.758	$6.36 \times 10^8$	
			10:00:00	0.585	0.576	$1.91 \times 10^9$	
			15:40:00	0.556	0.644	$3.18 \times 10^9$	

\* Does not include these points

## DOCUMENT CONTROL DATA - R &amp; D

(Security classification of title, body of abstract and indexing annotation must be entered when the overall report is classified)

1. ORIGINATING ACTIVITY (Corporate author) Arnold Engineering Development Center ARO, Inc., Operating Contractor Arnold Air Force Station, Tennessee		2a. REPORT SECURITY CLASSIFICATION UNCLASSIFIED	
		2b. GROUP N/A	
3. REPORT TITLE THE EFFECT OF PROTON IRRADIATION RATE ON THE SOLAR TRANSMITTANCE OF A THERMAL CONTROL BINDER MATERIAL			
4. DESCRIPTIVE NOTES (Type of report and inclusive dates) Final Report - November 4, 1969 to May 15, 1970			
5. AUTHOR(S) (First name, middle initial, last name) W. G. Kirby and D. W. Mills, Jr., ARO, Inc.			
6. REPORT DATE December 1970		7a. TOTAL NO. OF PAGES 34	7b. NO. OF REFS 8
8a. CONTRACT OR GRANT NO. F40600-71-C-0002		9a. ORIGINATOR'S REPORT NUMBER(S) AEDC-TR-70-257	
b. PROJECT NO.		9b. OTHER REPORT NO(S) (Any other numbers that may be assigned this report)	
c. Program Element 64719F		ARO-VKF-TR-70-283	
d.			
10. DISTRIBUTION STATEMENT This document has been approved for public release and sale; its distribution is unlimited.			
11. SUPPLEMENTARY NOTES Available in DDC		12. SPONSORING MILITARY ACTIVITY Arnold Engineering Development Center, Air Force Systems Command Arnold Air Force Station, Tenn. 37389	
13. ABSTRACT An experimental investigation was conducted to study the effect of proton irradiation rate on the solar transmittance of a silicone rubber under a $10^{-8}$ torr vacuum. Measurements were made with 150-kev protons at irradiation rates of $6.6 \times 10^{10}$ , $6.6 \times 10^{11}$ , $6.6 \times 10^{12}$ , and $6.6 \times 10^{13}$ protons/cm <sup>2</sup> /sec, and with 50-kev protons at irradiation rates of $6.6 \times 10^{11}$ and $6.6 \times 10^{12}$ protons/cm <sup>2</sup> /sec. The effect of vacuum on the solar transmittance of the test material was negligible. The solar transmittance of the material appeared to decrease with decreasing irradiation rate. The solar transmittance of all samples was a power law function of the total energy accumulated per unit area of the sample between total energy levels of $10^8$ and $10^{10}$ ergs/cm <sup>2</sup> /sec.			

14. KEY WORDS	LINK A		LINK B		LINK C	
	ROLE	WT	ROLE	WT	ROLE	WT
proton irradiation solar transmittance coatings (rubber) vacuum chambers						